Numerical Study of an Air Intake of a Cruise Missile in Subsonic Mach Regime

S PANI[1], K V MURALIDHARAN[2], SK MAHARANA[3]
[1] *Research Scholar, VTU, Belgaum, Karnataka*
[2] *Professor, Department of Mechanical Engineering Dept. MVJ College of Engineering, Bengaluru*
[3] *Professor, Dept. of Aeronautical Engineering, Acharya Institute of Technology, Bengaluru*

Abstract— Cruise missiles are low-altitude, fast-moving guided bombs that fly parallel to the ground. Due to the need for a low specific fuel consumption (SFC) to aid in travelling greater distances, a turbofan engine is employed to propel this type of missile. Because the power plant is an air breathing engine and the route is essentially terrain hugging, the air entrance to the engine must be properly let in. Inlets are crucial to the overall functioning of a jet engine and have a substantial impact on thrust output. As the plane speeds up, the inlet duct design becomes increasingly critical. The engine thrust would be great only if the inlet duct provided the required airflow at the maximum possible pressure. The work presented here is a study and design of an air intake for a conventional cruise missile in this direction. The goal of this research is to find the overall pressure recovery coefficient at the aerodynamic interface plane (AIP) by numerically simulating airflow via the air intake. Total pressure recovery has been determined quantitatively at different positions (0o to 360o) of AIP. The intensity of circumferential and radial distortions, as well as total pressure recovery (PR) coefficients for AIP, were then estimated. The maximum PR that may be achieved is 0.9. The flow was optimized using a genetic algorithm, with the corrected mass flow serving as the fitness function.

Indexed Terms-- Aerodynamic interface plane, , Distortions Specific fuel consumption, Total pressure recovery

I. INTRODUCTION

Cruise missiles are guided weapon systems that rely on aerodynamic forces to maintain their altitude. They are made up of four basic components: an airframe, a guidance system, a payload, and a propulsion system. Cruise missiles could be linked to small, pilotless planes if these crucial components are carefully studied [1-2]. Many studies have found that subsonic cruise with turbojet power has better range characteristics than the best alternative among the alternatives [3]. Maximum thrust [4] is achieved by reducing total pressure loss throughout the intake by delivering efficient dynamic pressure to static pressure transition. The ratio of total pressure at the aerodynamic interface plane (AIP) to free-stream total pressure is an intake performance metric called efficiency. The aerodynamic interface plane is an imaginary area located at the intersection of the turbojet engine's diffuser end and compressor face. NACA-style air intakes[5] have a trapezoidal opening and sharp lateral edges that generate two counter-rotating vortices and are flush with the airframe. The most prevalent and important parameter in the design of turbojet and turbofan engine intakes is pressure recovery[6]. The engine compressor's thrust and stability are affected by pressure recovery [7]. For the design process, a corrected value of the mass flow rate parameter is necessary in order to compare it for different flight situations and ambient conditions [8]. The distortion coefficient [9] is used to assess the flow quality within the intake. Wind tunnel testing is usually required after designing the intake duct to evaluate the air flow characteristics on the engine face. The impact of distortion on engine performance and stability under varied flying situations [10] is significant and large levels of distortion coefficient mean non-uniform pressure load on the compressor blades, which can damage compressor blade stability and induce surge, an aerodynamic stall. When specific distortion requirements at the aerodynamic interface plane (AIP) are met, the engine's compliance with the inflow circumstances is ensured [11]. The

circumferential distortion extent and distortion coefficients [12-13] have been investigated. Because of the nature of the technique, gradient-based optimization methods may be dangerous; the solution may converge in a local optimum rather than the global optimum [14]. Furthermore, the beginning point has a significant impact on convergence in these algorithms.

Stochastic methods, on the other hand, include some unpredictability to avoid convergence to a local optimum, and thus are less dependent on starting locations than gradient approaches. Stochastic methods, on the other hand, necessitate more iterations than gradient-based optimization techniques. Taking into account the simulation duration of high accuracy CFD tools and the starting point of optimization, which is regarded to be near the global optimum, the gradient based optimization approach is found to be the most suitable. A design objective function is determined for design optimization issues based on the design problem's aims.Multi-objective optimization issues, such as maximizing one design goal while minimizing another, are usually referred to as multi-objective optimization problems.

At the end of 1945, Frick et al. [15] introduced NACA-type submerged intake and issued a report about their experimental study based on it. Mossman and Randall [16] looked at the NACA submerged intake duct's major design characteristics. Entrance width to depth ratio, ramp wall divergence, ramp angle, and deflector size were the subjects of their experiments. Delany [17] did an experimental research on a 1/4 size model of a common fighter plane to see how submerged intake walls affected intake performance. At subsonic and transonic speeds, Mossman [18] studied the impact of side walls on submerged intake performance. Similar experimental work on the side-wall design for a NACA-type subsonic intake for transonic speeds was done by Taylor [19]. In order to investigate the influence of ramp divergence on pressure recovery, Martin and Holzhauser [20] conducted a NACA submerged air intake research on a full-scale model of a fighter jet. The effects of Mach number, angle of attack, entrance mass flow, boundary layer thickness, and intake position on the submerged intake performance are investigated experimentally by Hall and Frank [21]. In addition, considerable research was done on submerged intakes at various Mach regimes. Experimental examinations of submerged intake behavior at different Mach regimes at transonic and high subsonic speeds were carried out in references [22-24]. Before designing and optimizing a cruise missile's air intake, the design parameters must be known. The goal is to improve intake design by taking into account flow physics, operational conditions, and different flow regimes. The investigation will be conducted using both numerical and experimental methods. The very relevant parameters that affect the pressure recovery coefficients and circumferential and radial distortions will be discovered through the testing design. There is potential to widen the optimization using newer ways to arrive at an acceptable set of parameters because there is less research on this area. Because the cruise missile's air intake has so much room for improvement, new methodologies are required to better analyze the impact of various design parameters on intake performance at AIP. As a consequence of a series of simulations of flow through the intake under various operating conditions, the focus of this research is on optimization, with a particular emphasis on numerical analysis that aids in speedier decision making in the design of air intakes.

II. NUMERICAL SETUP AND APPROACH

The numerical approach entails creating a geometry with the model's dimensions, meshing it, and assigning the flow through the Intake's boundary conditions. The Intake model and its mesh view are presented in Fig.1 below. CATIA, a commercial modelling software, was used to model the air intake geometrically (Computer Aided Three-Dimensional Interactive Application). Figure 1 and 2 show the flow domain with the tetrahedral mesh.

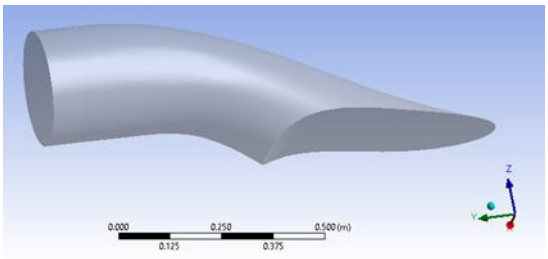

Fig.1 Numerical setup: CATIA model

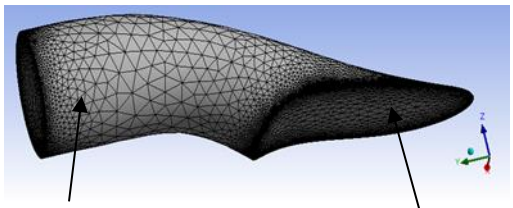

Fig.2 its meshed view used for numerical computation

VALIDATION OF THE NUMERICAL APPROACH

The numerical values of the pressure recovery (PR) ratio were validated. The numerical result derived from the present method was compared to the result (pressure recovery ratio versus Mach) described in Ref. [27], as shown in Fig.3. In Fig.4, the pressure recovery values for the Air Intake considered in this work have been displayed with respect to Mach number. The plots are only mentioned in Fig.4 (a) for the AIP area=0.06 m^2 (denoted by A) when Mach number is between 0.4 and 1.0. The change of pressure recovery with regard to Mach number when it is between 1 and 4 is shown in Fig.4(b).The goal is to show a comparison between Fig.3 and Fig.4, and to show that the overall trends in both cases (the current work and the reference) are similar, despite differences in predictor values. Given that both trials were conducted for different engines under various operating conditions, the variation trends are rather pleasing. The physics, however, stay the same, allowing for the confirmation of one of the most crucial quantities, PR.

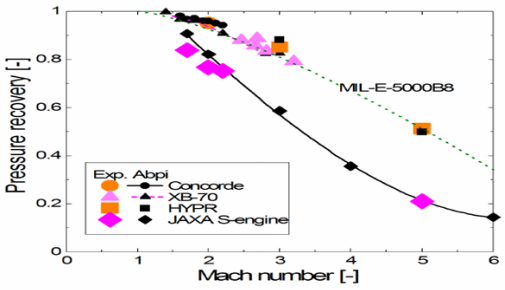

Fig.3 Variation of pressure recovery with respect to Mach number of the flow through Intake [19]

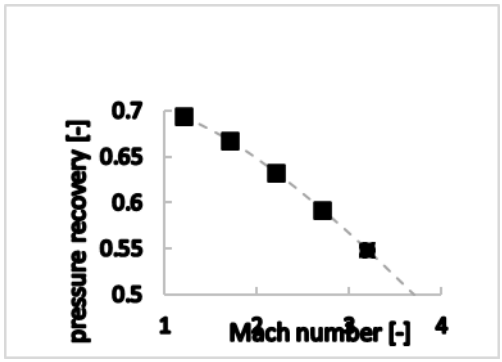

Fig.4 (a)

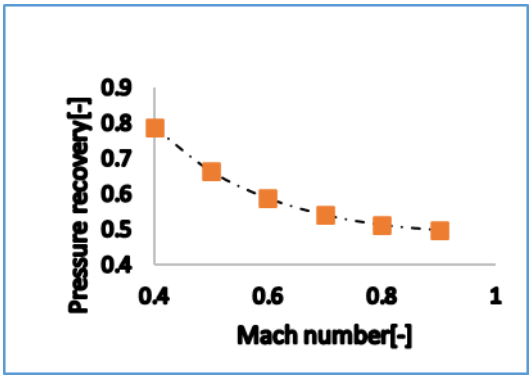

Fig4.(b)

Fig.4. (a) and (b) Variation of pressure recovery with respect to Mach number of the flow through Intake (present study)

III. RESULTS AND DISCUSSIONS

The study's purpose is to improve cruise missile intake design. The goal of the research is to calculate the pressure recovery ratio and distortions at AIP before optimizing the corrected mass flow rate at the same site. The optimization's objective function demands the primary variables that influence and contribute to the outcome of the optimization process. The objective function, which is a function of Mach number, total pressure, total pressure, and input outlet area, is the highest mass flow rate. The numerical simulation and genetic algorithm (GA) optimization findings are shown and discussed further down.

VELOCITY AND PRESSURE VARIATIONS IN INTAKE

The outlet and Aerodynamic Interface Plane (AIP) are the subjects of the study's predictions, as shown in

Fig.5. As a result, the pressure and velocity distributions inside the intake, along the walls, and at the outflow must all be considered. Similarly, pressure recovery at the AIP of the Intake has a substantial effect on mass flow rate. Mass flow rate, pressure recovery coefficient, and distortion coefficient are the most common parameters used to determine intake performance and stability.

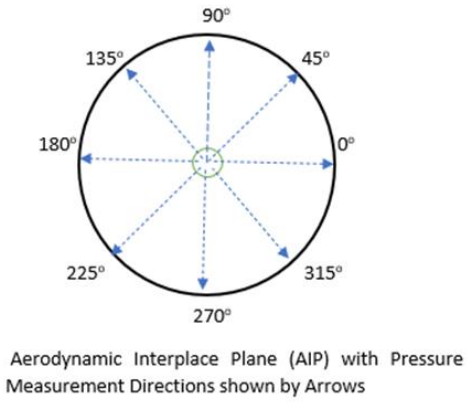

Fig. 5 Aerodynamics Interface Plane (AIP) with pressure measuring direction indicated by arrows

The AIP shown in the Fig.5 has pressure measuring directions indicated by arrows. The total pressure is measured at the designated pressure measuring points and each value is divided by the total pressure value(P_t) at sea level to find the pressure recovery rate ($P_{t,AIP}/P_{t,\ sea\ level}$).

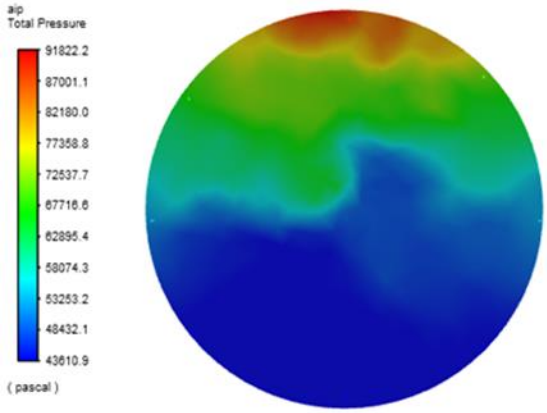

Fig. 6 Total pressure contours at the AIP

From the Fig.6 it is noted that the change of P_t. by 52% in AIP region with its highest value at 91.822 kPa and the lowest at 43.610 kPa. There is a possibility of flow distortion at AIP due to the wide gap between the pressure values. Because of this difference, there could be a significant difference in kinetic energy and hence a corresponding change in pressure energy between the inlet and outlet of Intake.

Below is shown in the Fig.7, the line diagram of AIP of the Air Intake where the pressure recovery coefficients have been computed. The location of a pressure measuring direction is measured in degrees using the symbol θ in anti-clockwise direction.

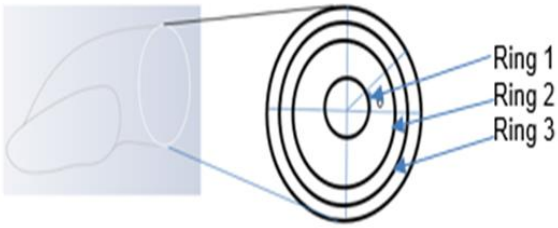

Fig.7 An illustration of AIP of Intake with 3 Rings

In Fig.8 is shown the averaged PR coefficient (P_t,AIP/P_t,sea) at different locations of a ring as depicted in the Fig.7. The highest averaged PR is observed at θ =270° and the lowest at θ = 90°.

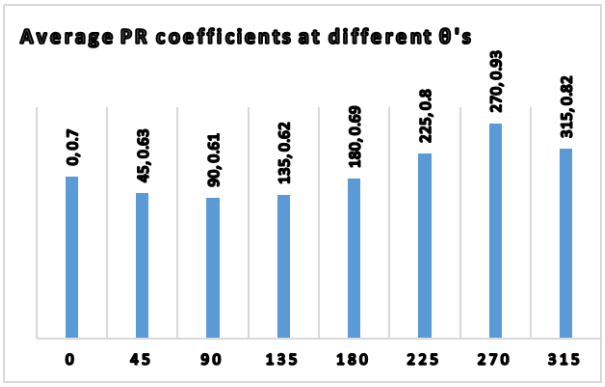

Fig.8 Average Pressure Recovery Coefficient

Circumferential distortion is noted from the study and reported below as intensity in the Fig.9. The intensity element, a numerical indication of the magnitude of pressure defect for a ring shown above, is computed as follows. The difference between the average value of total pressure for a ring(PAV) based upon the number of pressure measuring points and the average value of total pressure(PAVLOW) for the same ring

based only on the pressure readings that are below the ring average value divided by PAV is given as $Intensity = \frac{PAV - PAVLOW}{PAV}$ for a ring[25-26]. The highest value for the intensity in the present study is 0.3 and the lowest one is 0.17.

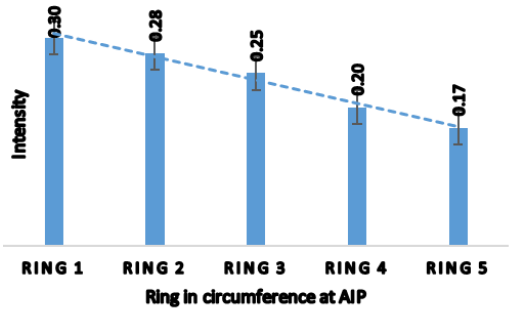

Fig.9 Intensity in each ring of AIP

Radial distortion is described in terms of the radial distortion intensity and is shown in Fig.10. This element indicates the difference between the ring average total pressure (PAV) and the face average total pressure (PFAV) normalised with the face average value[17-18]. Each ring on the same total pressure profile has its own value of radial distortion intensity. This parameter may take negative values as well when the ring average total pressure happens to be greater than the face average one.

$$Radial\ Intensity = \frac{PFAV - PAV}{PFAV}$$

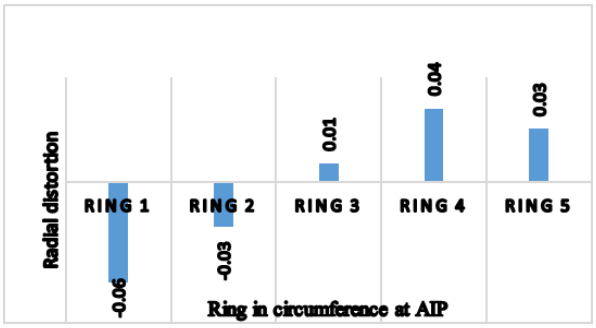

Fig.10 Radial distortion at each ring of AI

Genetic Algorithm Optimization

A genetic algorithm is a search heuristic that is inspired by Charles Darwin's theory of natural evolution. This algorithm reflects the process of natural selection where the fittest individuals are selected for reproduction in order to produce offspring of the next generation. The fitness function- the corrected mass requires the five design variables that are contributing to its maximization. The design variables are velocity of air, total temperature, total pressure, total pressure ratio and total temperature ratio.The corrected mass is given below.

$\dot{m}_{corrected} = \dot{m} * \frac{\sqrt{\frac{T_t}{T_{sea}}}}{\frac{P_{t,AIP}}{P_{sea}}}$, where $\dot{m} = \frac{AP_0}{\sqrt{T_0}}\sqrt{\frac{\gamma}{RT}}M\left[1 + \frac{\gamma-1}{2}M^2\right]^{-\frac{\gamma+1}{2(\gamma-1)}}$, total temperature is $T_0 = T\left[1 + \frac{\gamma-1}{2}M^2\right]$, total pressure is $P_0 = P\left[1 + \frac{\gamma-1}{2}M^2\right]^{\gamma/(\gamma-1)}$ and γ is the ratio of the specific heat of the gas at a constant pressure to its specific heat at a constant volume. The contraints used in the fitness function are the following:

Mach number , M<1.0, A_{AIP} is fixed and $\frac{P_{t,AIP}}{P_{sea}} < 1.0$ and $\frac{T_t}{T_{sea}} < 1.0$.

The selection function used in the optimisation is stochastic uniform.The mutation and crossover are constraints dependent. The optimisation process has converged(Fig.11) and the fitness function, in this case , the corrected mass is obtained for a specific combination of design parameters. Below is given the convergence plot of the GA optimisation. The best value obtained (the optised value) is 10 kg/sec. The number generations required for the convergence is noted as 150.

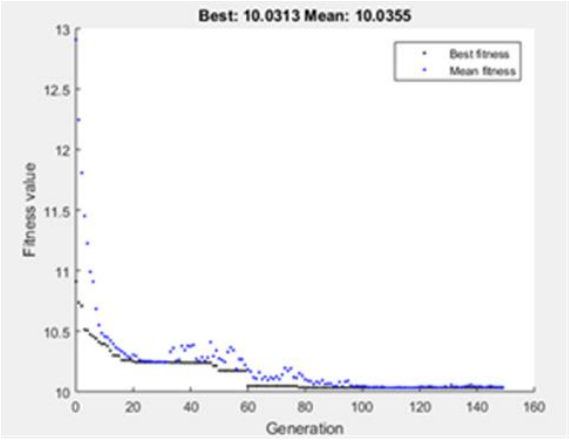

Fig.11 Convergence plot of genetic algorithm optimisation

Velocity=237 m/s, total temperature=325 K, total pressure=100.315 kPa, PR=0.9, and temperature ratio=1.0 are the optimised values for five design variables. The variation of corrected mass flow rate with respect to Mach number(M) is illustrated in Fig.12 for various total pressure ratios. For a given PR, it is observed that the corrected mass flow increases as M increases. However, for lower PR, the rise in adjusted mass flow rate is greater than for higher PR.

The variation of corrected mass flow rate with respect to M is illustrated in Fig.13 for various total temperatures.vFor a given Tt, it is observed that the adjusted mass flow increases as M grows.However, for lower T_t, the rise in corrected mass flow rate is greater than for higher T_t.

The variation of corrected mass flow rate with respect to PR for various values of A is illustrated in Fig. 14. For a given A, it is observed that the corrected mass flow reduces as PR increases.

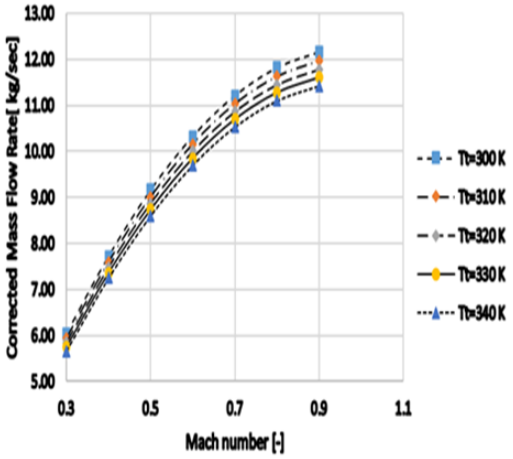

Fig.12 Corrected Mass Flow rate versus Mach No. at a specific PR

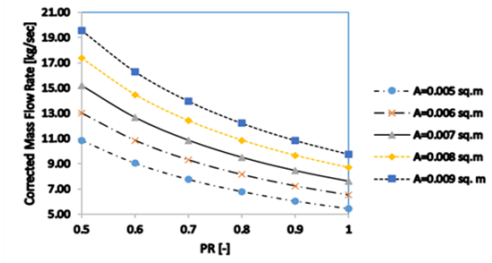

Fig 13 Corrected Mass Flow rate versus Mach No. at a specific Tt

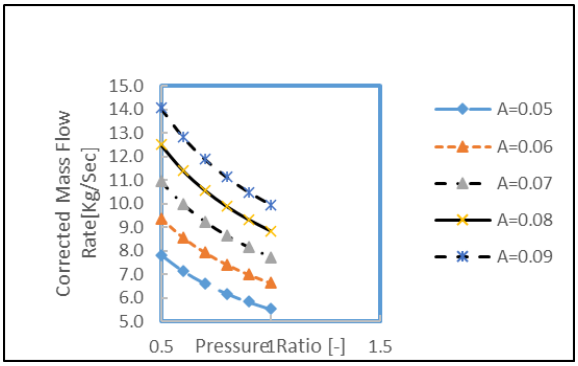

Fig.14 Corrected Mass Flow rate versus PR at different AIP area

IV. CONCLUSION

The flow inside a cruise missile's air intake has been numerically simulated. The grid independence analysis was conducted, and the variation between the identical variables obtained from three different grid configurations was shown to be less than 5%. The highest PR obtained was 0.9. The same pressure was employed as a design variable for the genetic algorithm (GA) optimization technique to optimize the adjusted mass flow rate. The greatest mass flow rate of 10.03 kg/sec was obtained. A performance analysis of the input was completed. At 270°, the average PR is highest, while at 90°, it is lowest. In this investigation, the greatest intensity value is 0.3, while the lowest is 0.17. For a given PR, it is also found that the adjusted mass flow increases as M grows. The adjusted mass flow increases as M increases for a given T^t, according to the research.

REFERENCES

[1] D. Tanks, "Assessing the Cruise Missile Puzzle: How great a defense challenge," The Institute for Foreign Policy Analysis, Washington DC.

[2] H. Avcıoğlu, "A Tool For Trajectory Planning and Performance Verification of Cruise Missiles," Middle East Technical University, Ankara, September, 2000.

[3] E. Fleeman, Tactical Missile Design, Reston, Virginia: AIAA Education Series, 2001.

[4] G. Laruelle, "Air Intakes: Role, Constrains and Design," International Council of the Aeronautical Sciences Congress, Les Mureaux, France, 2002.

[5] L. Hime, C. Perez and S. Ferreira, "Review of the Characteristics of The Submerged Inlets," 18th International Congress of Mechanical Engineering, Ouro Preto, MG, November 6-11, 2005.

[6] Oral Akman, Subsonic-transonic submerged intake design for a cruise missile, MS Thesis 2014.

[7] T. Reynolds, Flow Control Application in a Submerged Inlet Characterized by Three-Component LDV, Wright-Patterson Air Force Base, Ohio: Graduate School of Engineering and Management Air Force Institute of Technology Air University, 2010.

[8] J. D. Mattingly, Elements of Propulsion: Gas Turbines and Rockets, Blacksburg, Virginia: AIAA Education Series.

[9] J. D. Mattingly, W. H. Heiser and D. T. Pratt, Aircraft Engine Design, Alexander Bell Drive, Reston: AIAA Education Series, 2002.

[10] L. Kyungjae, L. Bohwa, K. Sanghun, S. Y. and D. L., "Inlet Distortion Test with Gas Turbine Engine in the Altitude Engine Test Facility," 27th AIAA Aerodynamic Measurement Technology and Ground Testing Conference, Daejeon, Korea, 28 June-1 July, 2010.

[11] M. Rütten, S. Kuckenburg, S. Koch and M. Rein, "Investigation of the Flow within Partially Submerged Scoop Type Air Intakes," AIAA Applied Aerodynamics Conference, San Diego, CA, 2013.

[12] SAE, "Aerospace Recommended Practive, Gas Turbine Engine Inlet Flow Distortion Guidelines, SAE ARP1420 Rev.B," SAE Aerospace International Group, USA, 2011.

[13] Bissinger and T. Breuer, "Basic Principles – Gas Turbine Compatibility – Intake Aerodynamic Aspects," Encyclopedia of Aerospace Engineering - Volume 8 - Chapter EAE487, Munich, Germany.

[14] E. S. Taskinoglu, A Multi objective Shape Optimization Study for A Subsonic Submerged Inlet, New Jersey : The State University of New Jersey , May 2004.

[15] C. Frick, W. F. Davis, L. M. Randall and E. A. Mossman, "An Experimental Investigation of NACA Submerged-Duct Entrances," National Advisory Committee for Aeronautics, Washington, 1945.

[16] E. Mosman and L. Randall, "An Experimental Investigation of the Design Variables For NACA Submerged Duct Entrances," National Advisory Committee for Aeronautics, Washington, 1948.

[17] N. Delany, "An Investigation of Submerged Air Inlets on a 1/4 Scale Model of a Typical Fighter-Type Airplane," National Advisory Committee for Aeronautics, Washington, June, 1948.

[18] E. A. Mossman, "A Comparison of Two Submerged Inlets at Subsonic and Transonic Speeds," National Advisory Committee for Aeronautics, Washington, September, 1949.

[19] R. A. Taylor, "Some Effects of Side-Wall Modifications on the Drag and Pressure Recovery of an NACA Submerged Inlet at Transonic Speeds," National Advisory Committee of Aeronautics, Washington, 1952.

[20] N. J. Martin and C. A. Holzhauser, "An Experimental Investigation at Large Scale of Several Configurations of NACA Submerged Air Intake," National Advisory Committee for Aeronautics, Washington, October, 1948.

[21] C. F. Hall and J. Frank, "Ram-Recovery Characteristics of NACA Submerged Inlets at High Subsonic Speeds," National Advisory Committee for Aeronautics, Washington, November, 1948.

[22] J. Axelson and T. R. A., "Preliminary Investigation of the Transonic Characteristics of an NACA Submerged Inlet," National Advisory Committee for Aeronautics, Washington, June, 1950.

[23] J. L. Frank, "Pressure-Distribution and Ram-Recovery Characteristics of NACA Submerged Inlets at High Subsonic Speeds," National Advisory Committee for Aeronautics, Washington, July, 1950.

[24] J. S. Dennard, "A Transonic Investigation of the Mass Flow and Pressure Recovery Characteristics of Several Types of Auxiliary Air Inlets," National Advisory Committee for Aeronautics, Washington, April, 1957.

[25] Technical Committee S-16, 1983, Inlet Total Pressure Distortion Considerations for Gas Turbine Engines, SAE AIR 1419, May 1983.

[26] SAE, 2002, Gas Turbine Engine Inlet Flow Distortion Guidelines, SAE AIR 1420, Rev B, 2002-02.

[27] Keiichi OKAI and Martin SIPPEL, 2nd European Conference for Aerospace Sciences (EUCASS), Component Analysis of TBCC Propulsion for a Mach 4.5 Supersonic Cruise Airliner January 2007.